

UC Merced

UC Merced Electronic Theses and Dissertations

Title

Greater temperature and precipitation extremes intensify Western US droughts, wildfire severity, and Sierra Nevada tree mortality

Permalink

<https://escholarship.org/uc/item/3t39d8jq>

Author

Crockett, Joseph L.

Publication Date

2017

Peer reviewed|Thesis/dissertation

UNIVERSITY OF CALIFORNIA, MERCED

Greater temperature and precipitation extremes intensify Western US droughts, wildfire severity, and Sierra Nevada tree mortality

A thesis submitted in partial satisfaction of the requirements for the degree Master of Science

in

Environmental Systems

by

Joseph L. Crockett

Committee in charge:

Professor Leroy Westerling, Ph.D. (Chair)

Professor Jessica Blois, Ph.D.

Professor Dan Cayan, Ph.D.

2017

Copyright

Joseph L. Crockett, 2017

All rights reserved

The Thesis of Joseph L. Crockett is approved, and is acceptable in quality and form for publication on microfilm and electronically:

Jessica Blois Date

Dan Cayan Date

Leroy Westerling (Chair) Date

University of California, Merced

2017

Dedication

I dedicate this thesis to my family, whose confidence and support never wavered; to Mary Martindale, whose passion for mountains and forests inspired my own; to Harry Robin, whose wise words directed me to the pursuit of science; to Ivy Price, whose strength and focus are daily inspirations; to my advisor, Leroy Westerling, whose tutelage expanded my abilities as a scientist; and to Richard Mwanza, for exemplifying care, work ethic, and hope of a better future.

Table of Contents

List of Figures	vi
Acknowledgements Page	vii
Abstract	viii

Thesis

Introduction	1
Methods	2
Results	4
Discussion/Conclusions	5
Figures	7
References	13

List of Figures

Figure 1. Drought location by duration/severity threshold combination, 1918 to 2014	7
Figure 2. Drought area (fraction) by year	8
Figure 3. Spatial footprints of selected droughts	9
Figure 4. Climatic Water Deficit (CWD), precipitation, and temperature in droughts	10
Figure 5. Monthly contributions of precipitation and temperature to CWD	11
Figure 6. Fire characteristics, 1984 to 2014 and tree mortality, 2009 to 2016	12

Acknowledgements

This research was supported by the California Nevada Applications Program under NOAA grant no. NA110AR4310150, the USDA Forest Service under award no. 14-CS-11052006-025, and the California Energy Commission under grant no. CEC-500-14-004. We thank D. Cayan, J. Blois, H. Preisler, D. Lettenmaier, and A. Keyser for their thoughtful comments; J. Milostan for assistance in processing hydroclimate data; and Z. Heath and H. Preisler for ADS mortality data. We thank H. Preisler for providing permission to reference their manuscript in review.

Any errors or omissions are our own.

Abstract

Joseph L. Crockett's M.S. thesis entitled, "Greater temperature and precipitation extremes intensify Western US droughts, wildfire severity, and Sierra Nevada tree mortality" was defended at University of California, Merced in 2017 with Dr. Leroy Westerling acting as committee chair. We analyzed gridded daily climate (temperature, precipitation and climatic water deficit) data to identify and characterize the spatiotemporal evolution of the largest Western United States droughts of the last 100 years. Droughts of the last 15 years (2000-2002, 2012-2014) had more extremes of climatic water deficit than earlier droughts, driven by greater temperature and precipitation extremes. Comparing fire extent and severity before, during and after drought events using the Monitoring Trends in Burn Severity dataset (1984-2014), we found fire size and high severity burn extent were greater during droughts than before or after. Similarly, recent Sierra Nevada forest mortality was greatest in drought-affected locations immediately after the drought. Climate simulations anticipate greater extremes in temperature and precipitation in a warming world: droughts and related impacts of the last 15 years may presage the effects of these extremes.

Introduction

Western United States (WUS) droughts may intensify with increasing temperatures and more variable precipitation as climate changes (Diffenbaugh et al. 2015, Ault et al. 2014). Presaging this future, the 2012-2014, and to a lesser extent the 2000-2003, drought were characterized by temperature and precipitation extremes, with severe consequences for vegetation, water supplies, agriculture, and wildfire risk (Guarín and Taylor 2005, Howitt et al. 2014, Parks et al. 2016). Although 2012-2014 conditions were unprecedented in the instrumental climate record, severe droughts occur periodically in the WUS (Griffen and Anchukaitis 2014). However, comparisons of spatiotemporal climate patterns over the formation, progression and termination of regional, multi-year WUS droughts remain scarce. Recent work offers substantive comparisons of droughts and effects, but these and similar studies can be spatially or temporally limited, or use indicators unsuited to assessing ecological impacts or long-term trends (Bachmair et al. 2016, Robeson et al. 2016, Ge et al. 2016, Asner et al. 2016).

Large-scale circulation patterns linked to global climate phenomena (e.g., ENSO, PDO, AMO) drive drought severity and extent, while local factors like topography modulate drought signatures (McCabe et al. 2004). In the West, highly variable climate, particularly precipitation, produces periodic interannual to decadal droughts (Cook et al. 2007, Routson et al. 2016, Griffen and Anchukaitis 2014). Large interannual droughts arise when conditions redirect storm paths over an extended period, with large ecosystem effects. For example, during the 2012 Californian drought, ENSO precursors developed into a persistent pressure ridge that redirected precipitation northward (Wang et al. 2014), resulting in progressive canopy water loss in 10+ million ha of forest (Asner et al. 2016). In the southwestern WUS in the 1950s and 2000s, high temperatures and disruption of summer precipitation exacerbated atmospheric moisture demand during droughts (Weiss et al. 2009), accompanied by greater rates of piñon pine mortality (Mueller et al. 2005) and bark beetle outbreaks (Shaw et al. 2005).

While ecosystems adapt to and arise from local long-term climate averages and variability, tolerance of seasonal drought in the arid West does not ensure survival during prolonged events (McDowell et al. 2008). Species adapted to mesic environments tend towards greater mortality during droughts, but survival of drought-tolerant species also decreases under severe and lengthy droughts (McDowell et al. 2008). Tree mortality due to drought stress, particularly during warmer periods, may result from hydraulic failure or carbon starvation, or indirectly through increased susceptibility to wildfire or biotic attack. Growing consensus indicates that greater tree mortality is occurring globally during “hot droughts” (Allen et al. 2009, Donat et al. 2016, Cook et al. 2014). However, commonly used temperature-insensitive drought indicators pose challenges to assessing the temperature-severity relationship (Williams et al. 2013).

Development of quantitative drought metrics that 1) capture the spatial scale of interannual droughts, 2) adjust for regional climate, topography, and demand, and 3) can be applied by a wide range of stakeholders is ongoing (Steinmann 2014). Limitations in drought metrics are unavoidable: severity is subjective beyond “dry” (Alley 1984, Bachmair et al. 2016). Stakeholder-specific thresholds identifying extreme aridity must be established, as drought indicators useful for one application may not be relevant to

another (Hayes et al. 2005, Stephenson 1998, Steinemann 2014, Bachmair et al. 2014). Optimal definitions of drought duration can be subjective (Ge et al. 2016): short durations may fail to differentiate seasonal climatological drought occurrence that ecosystems are adapted to from prolonged events with ecological significance. Alternatively, filtering for long duration may register “megadroughts” with decadal-scale duration, but obscure shorter droughts characteristic of the 20th century (Cook et al. 2007).

We use cumulative standardized climate water deficit (CWD) because of its strong links to vegetation distribution and temperature, applicability across spatial scales, and interpretability (Stephenson 1998, Lutz et al. 2010). CWD measures water imbalance and indicates cumulative unmet evaporative demand. Prolonged anomalous CWD can be interpreted as accumulated abnormal drying (Stephenson 1998). CWD incorporates soil, vegetation, temperature, precipitation, relative humidity and preceding conditions; thus, it is interpretable by stakeholders concerned with available precipitation (meteorological drought), moisture available for transpiration (agricultural drought), and moisture available as runoff (hydrological drought). CWD is sensitive to temperature, allowing assessment of effects of low precipitation coupled with rising temperatures during prolonged droughts (Stephenson 1998). Finally, consideration of secondary disturbances such as wildfire is facilitated because CWD is a suitable indicator of fire risk (Westerling 2016).

To place recent WUS drought in a long-term context, we compare the 2012 California drought to others over the last century, examining trends in drought severity measured by CWD. To illustrate how temperature and precipitation contributions to droughts vary over time, we disaggregate their influences on CWD over the course of the six largest droughts of the past century, with a specific focus on regions of extreme drought. Finally, we examine the effects of drought on wildfire size/severity and recent Californian tree mortality.

Methods

Data

Land Cover and Gridded Hydrological Data

We obtained $1/8^\circ$ gridded daily climate data (temperature and precipitation over 31°N to 49°N and -102°W to -125°W) derived from historical observations (1915-2014) using the index station method from the National Hydrologic Prediction System (NHPS) (Wood and Lettenmaier 2006). NHPS also provided daily simulations from the Variable Infiltration Capacity (VIC-3L) hydrologic model in water balance mode forced with gridded temperature and precipitation, fractional North American Land Data Assimilation System vegetation and topography, and climatological winds from NCEP reanalysis (Liang et al. 1994, Mitchell et al. 2004). VIC-3L simulations returned actual evapotranspiration (AET). We estimated potential evapotranspiration (PET) via the Penman-Monteith equation with the same forcing data (Penman 1948, Monteith et al. 1965), and calculated $\text{CWD} = \text{PET} - \text{AET}$ (Stephenson 1990). Monthly means (sums) were calculated for temperature (CWD and precipitation).

NHPS data end in 2014. To capture the full time-series of the 2012 drought

evolution, both before and after the drought, we obtained 2015 temperature and precipitation from the Livneh daily 1/16° meteorological dataset (Livneh 2015). We aggregated these to monthly values at the resolution of the VIC-3L variables. The 2015 CWD was simulated using the generalized additive model (GAM) discussed below. Correlations were strong between historical 1/8° VIC and rescaled Livneh data for monthly precipitation (0.920), temperature (0.995), and CWD (0.939).

Fire Severity Data

Fire records between January 1, 1984 and December 31, 2014 were accessed from the Monitoring Trends in Burn Severity (MTBS) project (MTBS 2016). MTBS assesses burn area and severity from pre- and post-disturbance satellite imagery (Eidenshink et al. 2007) for large (>400 ha) wildfires. We excluded prescribed or wild land use fires, leaving 7742 fires, and assigned each to the grid cell with greatest burned area coverage per fire to develop a 1/8° gridded fire history (Keyser and Westerling 2017).

Tree Mortality Data

We obtained 2.5 minute Aerial Detection Survey (ADS) counts of tree mortality (2004-2016) processed by Preisler et al. (in review) for California. ADS surveys tree mortality from bark beetles, wood borers and drought annually by air (Young et al. 2017). We aggregated tree mortality to our 1/8° grid and compared mortality before, during and after the 2012-2014 drought using non-parametric Kruskal-Wallis tests of ranks (KW test) followed by post-hoc Dunn's Tests between groups to determine significant shifts in distributions and extremes.

Drought Analysis

Drought Indicator

Standardized water-year CWD (October 1 through September 30) was used to classify pixels as drought if they met or exceeded a threshold (0.5, 1, 2 standard deviations above the 1918 to 2014 mean CWD) for a specified duration (2, 3, 5 years). A combination of duration and severity was selected that reduced small drought events while retaining a multiyear event centered on California beginning 2012.

Modeled Influence of Temperature and Precipitation

We developed a GAM to analyze effects of temperature and precipitation on CWD. GAMs are a non-parametric extension of generalized linear models. Models were built using the BAM function of the MGCV package in R (R Development Core Team 2008, Wood 2011) such that:

$$\text{CWD} = \beta_0 + f_1(\text{precipitation}) + f_2(\text{temperature}) + f_3(\text{lat, lon, month}) + \varepsilon \quad (1)$$

where CWD is the response, β_0 is the intercept, f_k are smooth functions estimated by

maximum likelihood, and precipitation, temperature, lat, lon, and month are explanatory variables. GAMs allow for non-linear relationships between response and covariates representing tradeoffs between a selected level of smoothing and allowed degrees of freedom. The model was fit to 75% of the data, leaving the remaining 25% for validation. A tensor smoother was applied to the spatial term as suggested by Aalto et al. (2013) and Wood (2006), while a cubic cyclic spline fit to month accounted for seasonality. Because CWD is calculated from P and T, we expected explained variance to be high and did not include other terms. We selected a GAM ($R^2 = 0.89$, correlation coefficient = 0.944) with separated terms to distinguish the influence of temperature vs. precipitation on monthly CWD during droughts (Wood 2006). To show accumulated effects, we cumulated temperature and precipitation influences over 36 months. To identify severe drought regions, we calculated the cumulative sums of CWD over 36 months (CWD36). We set an extreme severity threshold as the 95th percentile of the CWD36 over the six largest droughts.

High Severity Fire Models

MTBS classifies 30 meter pixels within fire perimeters into 6 severity classes: unburned to low, low, moderate, high, increasing greenness, and cloud cover/error. We categorized fires as “Before”, “During”, or “After” if they 1) occurred within a drought-affected area and 2) occurred in the preceding three years, during three-year drought window, or the following three years, respectively. The “After” class does not include post 2014 fires. We included fires from all drought grid cells (1984-2014) to extend the dataset. We compared fire size and fractions of fires that burned at low, medium, and high severity using KW tests followed by post-hoc Dunn’s tests between groups to determine significant shifts in distributions and extremes.

Results

We found no droughts at the most severe/longest duration (2 stan. dev./5 yr), while at the lowest severity/shortest duration (0.5 stan. dev./2 yr) the entire spatial domain was affected by drought at some point during the century (Fig. 1). We selected parameters of 1 standard deviation and three year duration for further analysis (Fig. 2). The six severe droughts identified represent different ecoregions and time periods, although some overlap occurred: the Pacific Northwest 1929-1931; Northern Rockies, 1934-1936; Southwest, 1954-1956; Interior, 1959-1961; Southern Rockies, 2000 to 2002; and Great Basin and California, 2012-2014 (Fig. 3). Three-year drought area was greatest in 2012-2014 (7%), followed by 1929-1931 (6.1%) and 1934 -1936 (5.39%).

Patterns across droughts included depressed precipitation relative to preceding and/or following years (Fig. 4a, 4c). First drought year was often characterized by elevated temperatures which subsequently declined, excepting the 2012-2014 drought, which started high and rose through 2015 (Fig. 4b). Parts of the 1934-1936 and 2012-2014 droughts appeared to extend into a fourth year: nearly 54% of both droughts exceeded 1 standard deviation CWD following the drought (in 1937 and 2015, respectively). 1937 is further characterized by depressed precipitation, though

temperature fell below the long-term average from a significantly high first drought year. In contrast, 2015 is characterized by near-normal precipitation and a continuing high temperature trend that began in the first drought year. In 2003, 37% of the 2000-2002 drought core region was as severe as 2002 and characterized by depressed precipitation and high temperature.

Precipitation contributions to CWD were similar between droughts, though median values differed (KW test, p -value < 0.01 , Fig. 5a). Temperature contributions were more variable and roughly comparable to the mean temperature experienced in droughts, i.e., high temperatures corresponded with high temperature contribution to CWD (Figs. 4, 5a). Both temperature and precipitation contributions in 2012-2014 exceed other droughts, especially considering the number and range of outliers (KW test, $p < 0.01$, $p < 0.01$) (Fig. 5a). Note that the spread of temperature and precipitation contributions to CWD differs significantly between droughts, from a near-neutral accumulated temperature contribution during 1929 to 1931 to wider spreads in conditions across the 1934 to 1936, 2000 to 2002, and 2012 to 2014 droughts. These differences are magnified in the most severe regions of each drought (Fig. 5b). Though similar in spatial extent (Fig. 3), earlier droughts are characterized by smaller variance of temperature and precipitation contributions (Fig. 5a) as well as smaller extremely severe regions, relative to 2012-2014 (Fig. 5b). The extreme 2012-2014 region has median temperature (precipitation) contributions 35% (102%) greater than earlier droughts, with extremes affecting a much larger area (Figs. 5b, c). The most severe instances were seen in the Sierra Nevada and Wasatch Range, highlighting the impact of sustained severe drought in watersheds (Cayan & Dettinger 2001, Udall & Overpeck 2017) (Figs. 3, 5b).

Total and high severity burned area were greater during droughts than before or after. Of 1932 large wildfires between 1984-2014 in cells affected by drought, 868 occurred in the three years preceding a drought, 820 occurred during, and 244 in the three years following. Fire size in drought pixels ranged up to 228,687 ha, compared to maximum size of 66,919 and 10,790 ha before and after, respectively. The 95th percentile of low and moderate severity burn fraction did not significantly differ from each other (KW test, $p > 0.05$, $p > 0.05$), while drought fires accounted for a 26.97% and 61.32% increase at the 95th percentile of high severity and total burn area respectively (KW test, $p < 0.01$, $p < 0.1$) (Fig. 6a). Fires in years following drought had greater moderate severity area, while years prior to drought had greater low severity area (Fig. 6a).

Tree mortality was greater across California following 2014 (KW test, $p < 0.05$) (Fig. 6b). In the periods preceding, during, and following the 2012-2014 drought mortality was greater in drought-affected areas (Dunn's test, $p < 0.05$, $p < 0.05$, $p < 0.05$).

Discussion/Conclusions

Climate projections anticipate warming temperatures for the next century, and although less certainty is attributed to precipitation, extreme high precipitation events may be separated by longer periods of aridity (Wuebbles et al. 2014). Though average standardized precipitation anomalies were similar across all droughts (Fig. 3), there were

more and greater precipitation extremes as well as temperature extremes in 2012-14 (Fig. 5a). Among the largest and most severe of the last century, the 2000-2002 and 2012-2014 droughts may be early analogs for climate change-enhanced droughts of the 21st century, particularly in regions with historically greater snowpack (Cook et al. 2015).

Of critical concern to land managers are recent increasing fire size and severity and tree mortality linked to increasing temperatures and aridity (Miller & Safford 2013, van Mantgem et al. 2013, Westerling 2016, Keyser and Westerling 2017, Young et al. 2017). Our results support multi-year severe drought as a factor in increasing fire size and severity, as well as tree mortality. Increased prevalence of dead or desiccated fuels from direct and indirect drought effects (Mueller et al. 2005, Shaw et al. 2005, McDowell et al. 2008) is conducive to crown fires, which require ladder fuels to move from volatile grasses to the less volatile mid-level forest to the dry and volatile canopy cover (Wagner 1977). In non-drought years, fires may be smaller and less severe because mid-level vegetation does not ignite and spread into the canopy cover as easily as following multiple years of desiccation. Temporal limitations of the MTBS record require conclusions be drawn from a period with increased fire size and frequency (Westerling 2016), but recent droughts encompassed the largest WUS fires during the last 30 years.

Tree mortality in California is a visual indicator of drought to the public. Our results indicated that greater mortality during the 2009 to 2016 period occurred in drought-affected than outside drought-affected areas, consistent with global trends (Allan et al. 2009, van Mantgem et al. 2013). The lagged temporal relationship between drought and tree mortality seen in Figure 6 has been noted in other drought events, with mortality possible decades later (Bigler et al. 2007). Extensive mortality occurred during the mid-1930s and early 2000s droughts, which we found to have similar temperature extremes and influence on CWD (Figs. 4b, 5a) (Albertson & Weaver 1945, Mueller et al. 2005).

While droughts recur throughout WUS history, droughts of the past 15 years were more intense than early-mid 20th century droughts, with greater temperature and precipitation extremes contributing to extreme CWD over a larger area. Land managers should anticipate droughts in the future similar to recent events and prepare for larger, more severe fires and greater tree mortality.

Figures

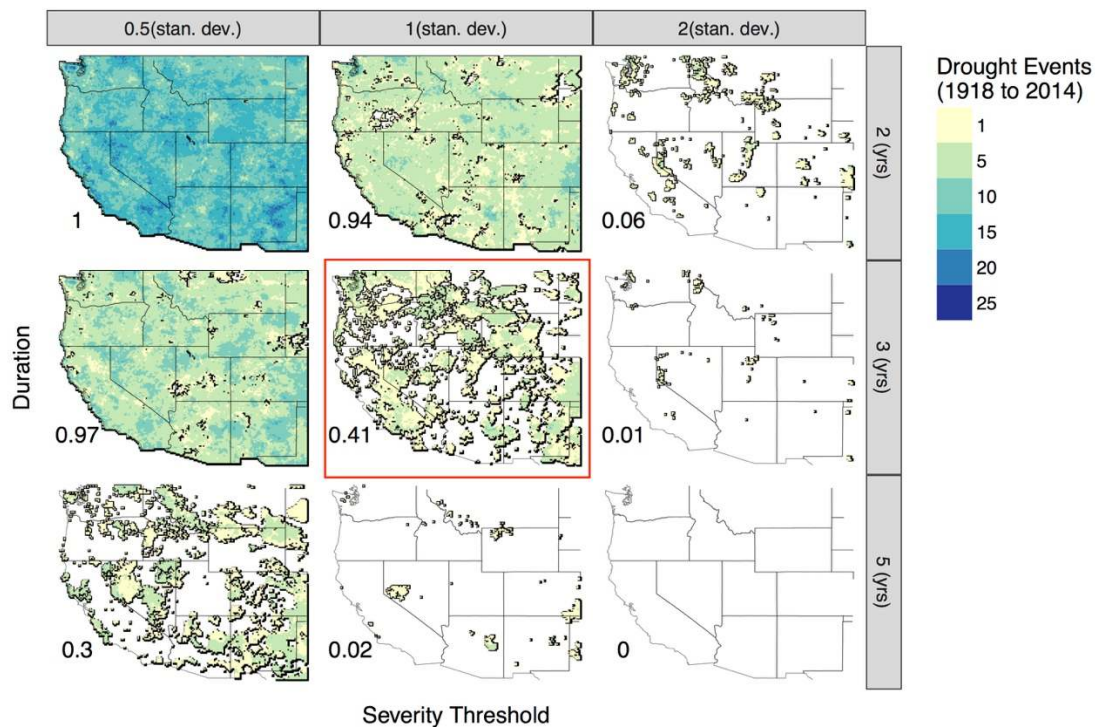


Figure 1. Spatial footprints of droughts are plotted by duration/threshold combination, 1918 to 2014. The location and frequency of drought occurrences are indicated by the color gradient. Area covered by drought (fraction) is shown in the lower left corner of plots. Our intention was to determine a combination of duration and threshold severity that reveals low drought frequency while retaining spatially extensive signals. This was best represented by a three year duration and 1 stan. dev. threshold (red box).

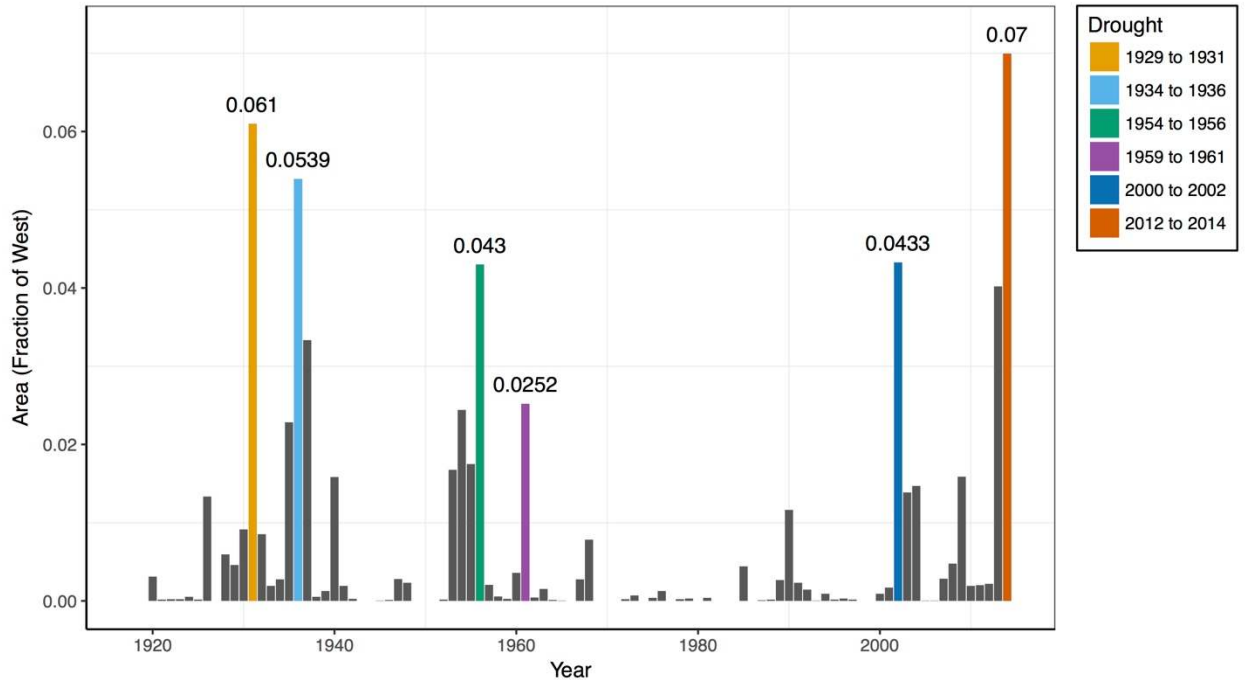


Figure 2. Drought area by year using a three year duration and 1 stan. dev. severity threshold is plotted by the third year identity. The x-axis is in years and the y-axis indicates drought cover for a given year (fraction of region). Bars are positioned on the third year of the drought window. Six droughts were selected for further analysis from 3 distinct periods: the 1930s, the 1950s, and the 2000s. Drought area for these six droughts are indicated by the fraction above the colored bars.

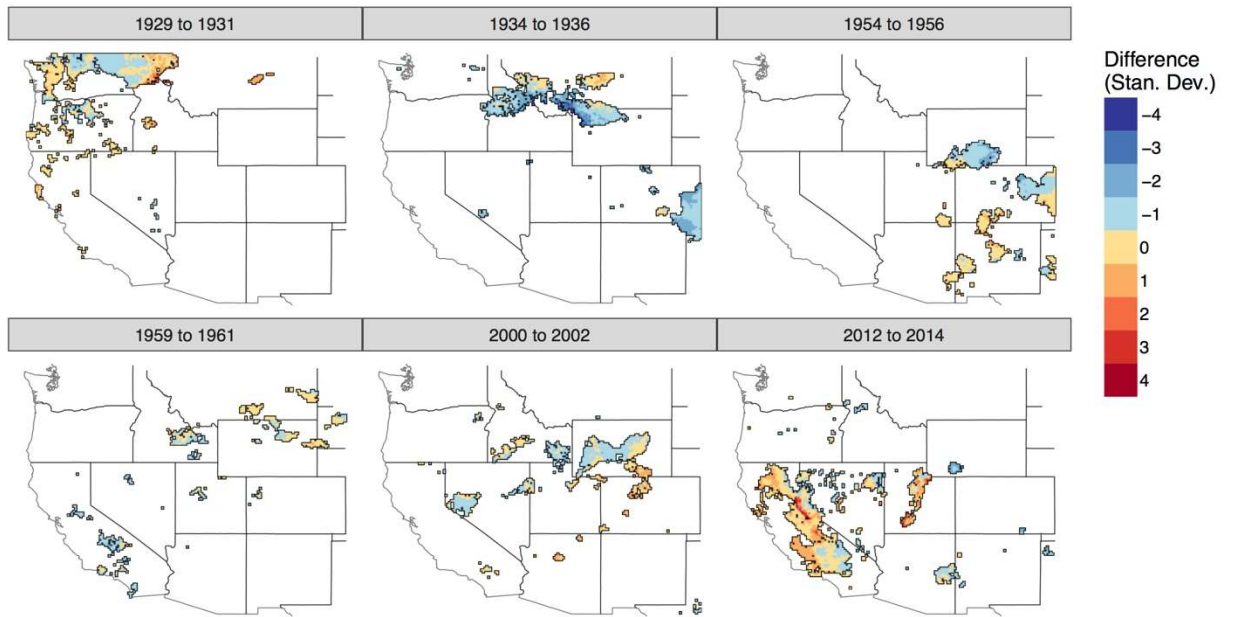


Figure 3. Spatial footprints of selected droughts are plotted with a color gradient indicating the strength of difference between the first and third water year CWD. The direction of the change (Red = drier, Blue = wetter) reveals the increasing or decreasing accumulated drought stress.

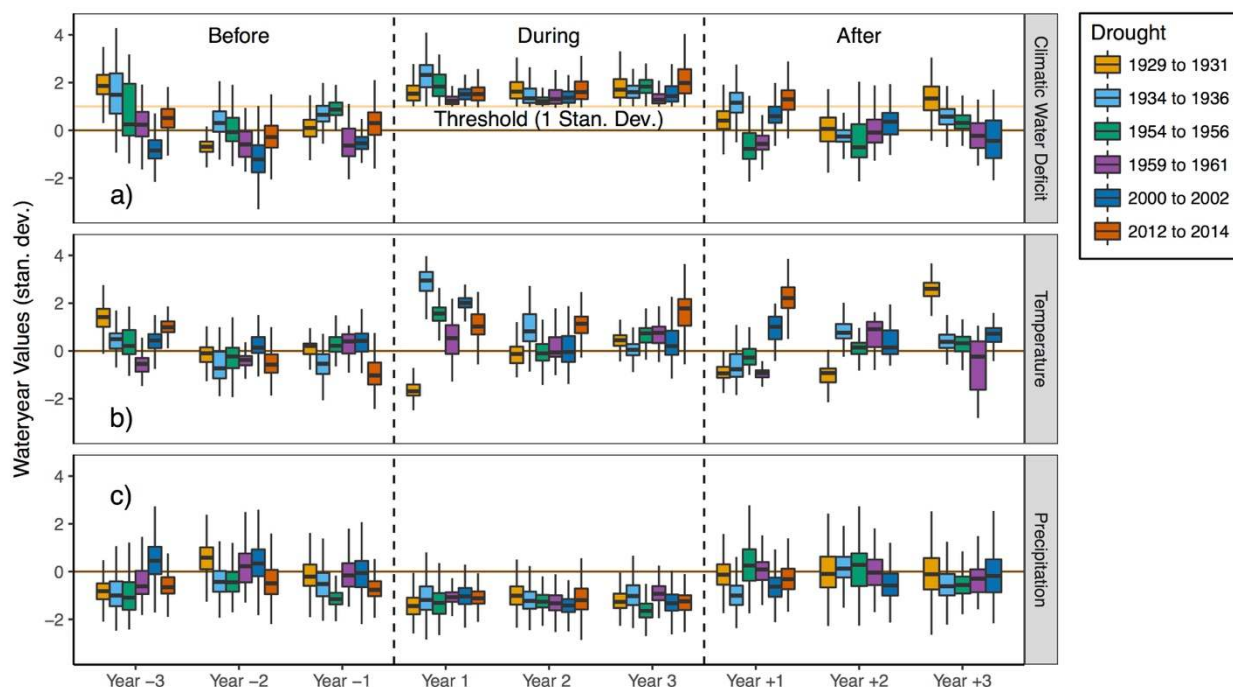


Figure 4. Water year standardized CWD, Precipitation, and Temperature in drought footprints are plotted preceding, during, and following selected drought events. Year -3 on the x-axis corresponds to three years before the beginning of the drought while Year +3 corresponds to the third year following the end of the drought. Boxplots describe the 25th to 75th percentile with medians shown by black horizontal lines and colored by drought. Whiskers are within $1.5 * IQR$. The 2012 to 2014 box (orange) in Year +1 indicates the added values from the Livneh meteorological dataset described in the text.

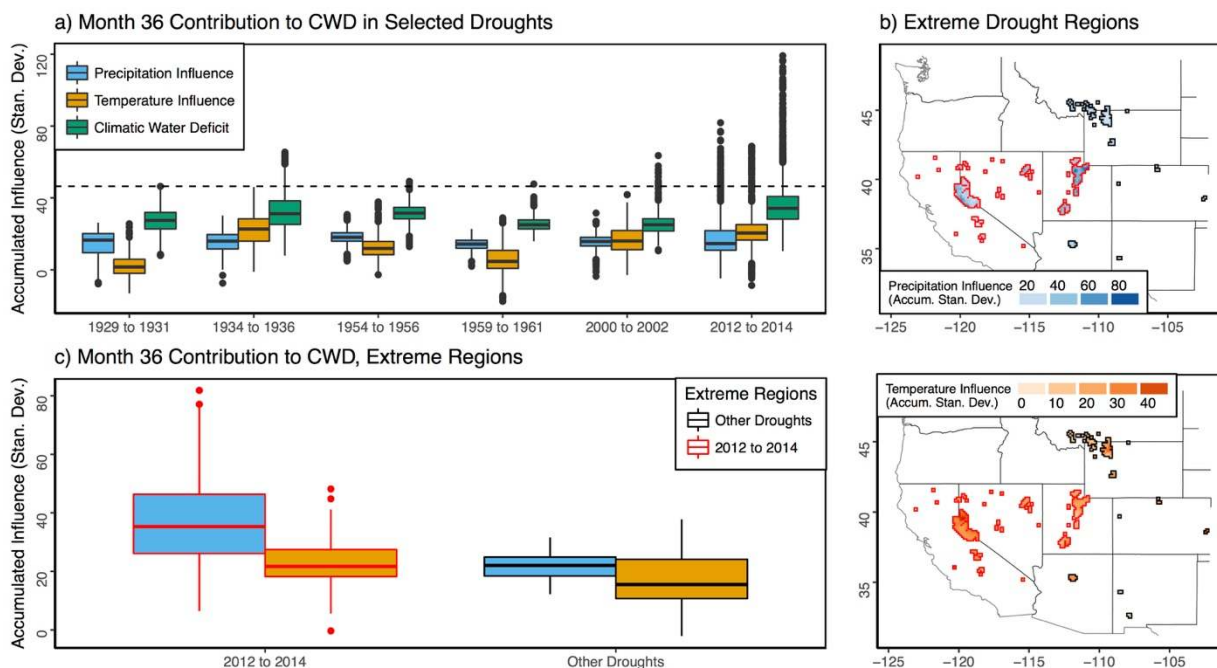


Figure 5. The accumulated relative monthly contributions of Precipitation and Temperature to CWD are plotted at the final month of drought. Plot a) shows boxplots of the 36th month precipitation contributions, temperature contributions, and CWD (PI36, TI36, and CWD36, respectively) in selected droughts. Boxplots describe the 25th to 75th percentile with medians shown by black horizontal lines and colored by drought. Whiskers are within $1.5 * IQR$. The dashed horizontal line indicates a single extreme severity threshold, calculated as the 95th percentile of the CWD36 from the six selected droughts. Plot b) shows the extreme drought area, with 2012 to 2014 extreme severity outlined in red and other droughts outlined in black. Plot c) shows boxplots of PI36 and TI36 in the extreme drought areas with colors corresponding to plot a) boxplot colors.

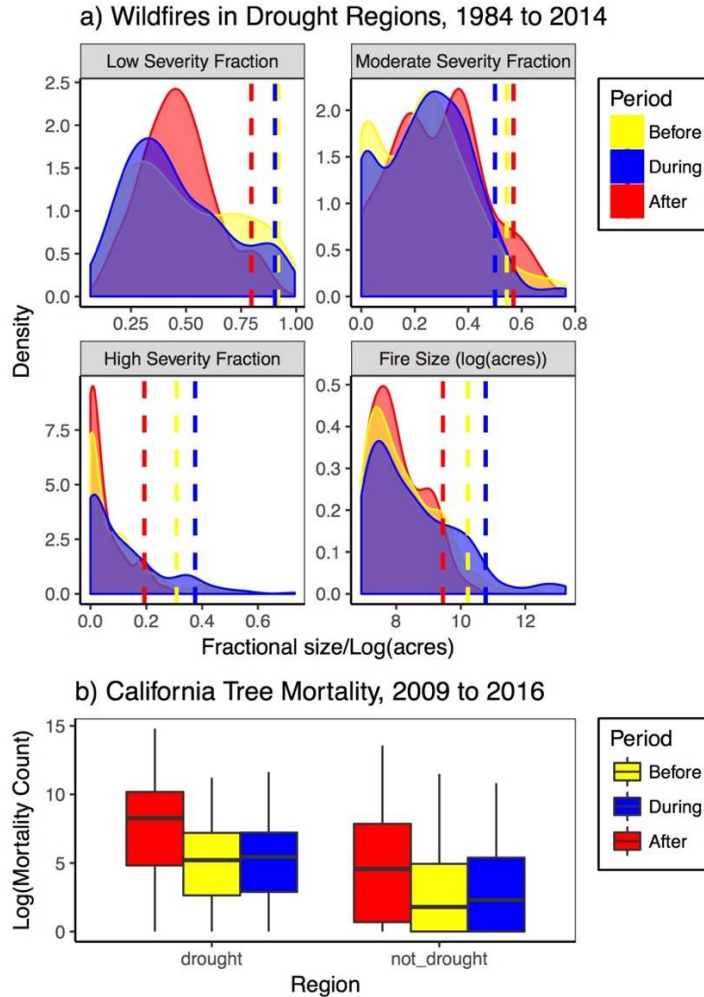


Figure 6. Recent drought effects on fire between 1984 and 2014 in the western United States (a) and California tree mortality between 2009 and 2016 (b). In a), Fire size and severity fraction of fires in three year periods preceding, during, and following droughts between 1984 and 2014, with the 95th percentile indicated by vertical lines. Severity is expressed as the fraction burned at a given severity in a fire and fire size is expressed as log-transformed burn acreage. Only non-management fires that burned larger than 1000 acres were included. In b), boxplots are divided into period (colors) and drought/non-drought areas (x-axis). The before period covers 2009 to 2011, the during period covers 2012 to 2014, and the after period covers 2015-2016. The y-axis is expressed in terms of log- transformed counts of tree mortality.

References

- Aalto, J., P. Pirinen, J. Heikkinen, and A. Venäläinen, 2013: Spatial interpolation of monthly climate data for Finland: comparing the performance of kriging and generalized additive models. *Theor. Appl. Climatol.*, **112** (1-2), 99–111.
- Albertson, F.W., Weaver, J.E., 1945. Injury and death or recovery of trees in prairie climate. *Ecol. Monogr.* **15**, 393–433
- Allen, C.D., Macalady, A.K., Chenchouni, H., Bachelet, D., McDowell, N., Vennetier, M., Kitzberger, T., Rigling, A., Breshears, D.D., Hogg, E.T. and Gonzalez, P., 2010. A global overview of drought and heat-induced tree mortality reveals emerging climate change risks for forests. *For. Ecol. Manage.*, **259** (4), 660-684.
- Alley, W. M., 1984: The palmer drought severity index: limitations and assumptions. *J. Climate. Appl. Meteor.*, **23** (7), 1100–1109.
- Asner, G. P., P. G. Brodrick, C. B. Anderson, N. Vaughn, D. E. Knapp, and R. E. Martin, 2016: Progressive forest canopy water loss during the 2012–2015 California drought. *Proc. Natl. Acad. Sci. U. S. A.*, **113** (2), E249–E255.
- Ault, T. R., J. E. Cole, J. T. Overpeck, G. T. Pederson, and D. M. Meko, 2014: Assessing the risk of persistent drought using climate model simulations and paleoclimate data. *J. Climate.*, **27** (20), 7529–7549.
- Bachmair, S., and Coauthors, 2016: Drought indicators revisited: the need for a wider consideration of environment and society. *Wiley Interdiscip. Rev.: Water*, **3** (4), 516–536.
- Bigler, C., Gavin, D. G., Gunning, C., & Veblen, T. T. (2007). Drought induces lagged tree mortality in a subalpine forest in the Rocky Mountains. *Oikos*, **116** (12), 1983-1994.
- Cayan, D. R., M. D. Dettinger, S. A. Kammerdiener, J. M. Caprio, and D. H. Peterson, 2001: Changes in the onset of spring in the western United States. *Bull. Amer. Meteor. Soc.*, **82** (3), 399–415.
- Cook, B. I., T. R. Ault, and J. E. Smerdon, 2015: Unprecedented 21st century drought risk in the American southwest and central plains. *Sci. Adv.*, **1** (1), e1400 082.
- Cook, B. I., J. E. Smerdon, R. Seager, and E. R. Cook, 2014: Pan- continental droughts in North America over the last millennium. *J. Climate.*, **27** (1), 383–397.
- Cook, E. R., R. Seager, M. A. Cane, and D. W. Stahle, 2007: North American drought: reconstructions, causes, and consequences. *Earth-Sci. Rev.*, **81** (1), 93–134.
- Diffenbaugh, N. S., D. L. Swain, and D. Touma, 2015: Anthropogenic warming has increased drought risk in California. *Proc. Natl. Acad. Sci. U. S. A.*, **112** (13), 3931–3936.
- Donat, M. G., A. D. King, J. T. Overpeck, L. V. Alexander, I. Durre, and D. J. Karoly, 2016: Extraordinary heat during the 1930s us dust bowl and associated large-scale conditions. *Climate. Dyn.*, **46** (1-2), 413–426.

- Eidenshink, J., B. Schwind, K. Brewer, Z. Zhu, B. Quayle, and S. Howard, 2007: A project for monitoring trends in burn severity. *Fire Ecol.* **3** (1): 3-21.
- Ge, Y., T. Apurv, and X. Cai, 2016: Spatial and temporal patterns of drought in the continental us during the past century. *Geophys. Res. Lett.*, **43** (12), 6294–6303.
- Griffin, D., and K. J. Anchukaitis, 2014: How unusual is the 2012–2014 California drought? *Geophys. Res. Lett.*, **41** (24), 9017– 9023.
- Guarín, A., and A. H. Taylor, 2005: Drought triggered tree mortality in mixed conifer forests in Yosemite national park, California, USA. *For. Ecol. Manage.*, **218** (1), 229–244.
- Hayes, M. J., L. F. Cavalcanti, and A. C. Steinemann, 2005: Drought indicators and triggers. *Drought and water crises: Science, technology, and management issues*, Donald A. Wilhite, Ed., CRC Press, 71–92.
- Howitt, R.E., Medellin-Azuara, J., MacEwan, D., Lund, J.R. and Sumner, D.A. 2014. Economic Analysis of the 2014 Drought for California Agriculture. Center for Watershed Sciences, University of California, Davis, California., Accessed 5 May 2016. [Available online: <http://watershed.ucdavis.edu>].
- Keyser, A.R. & Westerling, A.L. In press: 2017. Climate drives inter-annual variability in probability of high severity fire occurrence in the western United States. Accepted: *Environ. Res. Lett.*
- Liang, X., D. P. Lettenmaier, E. F. Wood, and S. J. Burges, 1994: A simple hydrologically based model of land surface water and energy fluxes for general circulation models. *J. Geophys. Res.: Atmos.*, **99** (D7), 14 415–14 428.
- Livneh, B., T. J. Bohn, D. W. Pierce, F. Munoz-Arriola, B. Nijssen, R. Vose, D. R. Cayan, and L. Brekke, 2015: A spatially comprehensive, hydrometeorological data set for Mexico, the US, and southern Canada 1950–2013. *Sci. Data*, **2**.
- Lutz, J. A., J. W. van Wagendonk, and J. F. Franklin, 2010: Climatic water deficit, tree species ranges, and climate change in Yosemite national park. *J. Biogeogr.*, **37** (5), 936–950.
- McCabe, G. J., M. A. Palecki, and J. L. Betancourt, 2004: Pacific and Atlantic Ocean influences on multidecadal drought frequency in the United States. *Proc. Natl. Acad. Sci. U. S. A.*, **101** (12), 4136–4141.
- McDowell, N., and Coauthors, 2008: Mechanisms of plant survival and mortality during drought: why do some plants survive while others succumb to drought? *New Phytol.*, **178** (4), 719–739.
- Miller, J. D., and H. Safford, 2012: Trends in wildfire severity: 1984 to 2010 in the Sierra Nevada, Modoc Plateau, and Southern Cascades, California, USA. *Fire Ecol.*, **8** (3), 41–57.
- Mitchell, K. E., and Coauthors, 2004: The multi-institution North American land data assimilation system (NLDAS): Utilizing multiple GCIP products and partners in a continental distributed hydrological modeling system. *J. Geophys. Res.: Atmos.*, **109** (D7).

- Monteith, J. L. (1965). Evaporation and environment. In *Symp. Soc. Exp. Biol* **19** (205-23), 4.
- MTBS Data Access: Fire Level Geospatial Data. MTBS Project (USDA Forest Service/U.S. Geological Survey). Accessed 8 October 2016. [Available online: <http://mtbs.gov/data/individualfiredata.html>].
- Mueller, R. C., C. M. Scudder, M. E. Porter, R. Talbot Trotter, C. A. Gehring, and T. G. Whitham, 2005: Differential tree mortality in response to severe drought: evidence for long-term vegetation shifts. *J. Ecol.*, **93** (6), 1085–1093.
- Parks, S. A., C. Miller, J. T. Abatzoglou, L. M. Holsinger, M.-A. Parisien, and S. Z. Dobrowski, 2016: How will climate change affect wildland fire severity in the Western US? *Environ. Res. Lett.*, **11** (3), 035002.
- Penman, H. L., 1948: Natural evaporation from open water, bare soil and grass. *Proc. R. Soc. A.*, **193**, 120–145.
- Preisler, H. K., Grulke, N. E., Heath, Z., Smith, S. L., in review, Analysis and out-year forecast of beetle, borer, and drought-induced tree mortality in California.
- R. Development Team 2011: R: A language and environment for statistical computing. *Vienna: R Foundation for Statistical Computing*.
- Robeson, S. M. (2015), Revisiting the recent California drought as an extreme value, *Geophys. Res. Lett.*, **42**, 6771–6779, doi:10.1002/2015GL064593.
- Routson, C. C., C. A. Woodhouse, J. T. Overpeck, J. L. Betancourt, and N. P. McKay, 2016: Teleconnected ocean forcing of western North American droughts and pluvials during the last millennium. *Quat. Sci. Rev.*, **146**, 238–250.
- Shaw, J. D., B. E. Steed, and L. T. DeBlander, 2005: Forest inventory and analysis (FIA) annual inventory answers the question: What is happening to pinyon-juniper woodlands? *J. For.*, **103** (6), 280–285.
- Steinemann, A., 2014: Drought information for improving preparedness in the western states. *Bull. Amer. Meteor. Soc.*, **95** (6), 843–847.
- Stephenson, N., 1998: Actual evapotranspiration and deficit: biologically meaningful correlates of vegetation distribution across spatial scales. *J. Biogeogr.*, **25** (5), 855–870.
- Stephenson, N. L., 1990: Climatic control of vegetation distribution: the role of the water balance. *Amer. Nat.*, **135** (5), 649–670.
- Udall, B. and J. Overpeck (2017), The twenty-first century Colorado River hot drought and implications for the future, *Water Resour. Res.*, **53**.
- van Mantgem, P. J., J. C. Nesmith, M. Keifer, E. E. Knapp, A. Flint, and L. Flint, 2013: Climatic stress increases forest fire severity across the western United States. *Ecol. Lett.*, **16** (9), 1151–1156.

- Wagner, C. V., 1977: Conditions for the start and spread of crown fire. *Can. J. For. Res.*, **7** (1), 23–34.
- Wang, S.-Y., L. Hipps, R. R. Gillies, and J.-H. Yoon, 2014: Probable causes of the abnormal ridge accompanying the 2013–2014 California drought: ENSO precursor and anthropogenic warming footprint. *Geophys. Res. Lett.*, **41** (9), 3220–3226.
- Weiss, J. L., C. L. Castro, and J. T. Overpeck, 2009: Distinguishing pronounced droughts in the southwestern United States: Seasonality and effects of warmer temperatures. *J. Climate*, **22** (22), 5918–5932.
- Westerling, A. L., 2016: Increasing western US forest wildfire activity: sensitivity to changes in the timing of spring. *Phil. Trans. R. Soc. B*, **371** (1696), 20150178.
- Williams, A. P., and Coauthors, 2013: Temperature as a potent driver of regional forest drought stress and tree mortality. *Nat. Clim. Change*, **3** (3), 292–297.
- Wood, A. W., and D. P. Lettenmaier, 2006: A test bed for new seasonal hydrologic forecasting approaches in the western United States. *Bull. Amer. Meteor. Soc.*, **87** (12), 1699–1712.
- Wood, S., 2006: *Generalized Additive Models: An Introduction with R*. CRC press.
- Wood, S. N., 2011: Fast stable restricted maximum likelihood and marginal likelihood estimation of semi-parametric generalized linear models. *J. R. Stat. Soc. B (Stat. Methodol.)*, **73** (1), 3–36.
- Wuebbles, D., and Coauthors, 2014: CMIP5 climate model analyses: climate extremes in the United States. *Bull. Amer. Meteor. Soc.*, **95** (4), 571–583.
- Young, D. J. N., Stevens, J. T., Earles, J. M., Moore, J., Ellis, A., Jirka, A. L., Latimer, A. M., 2017: Long-term climate and competition explain forest mortality patterns under extreme drought. *Ecol. Lett.* **20**, 78–86.